

Figure 1. Earth- Sun angles: declination  $\delta$ , hour angle  $\omega$ , altitude  $\alpha$ , azimuth  $\psi$ , zenith  $\theta$ , latitude  $\phi$ .

### 3. THE NORMAL UNIT VECTOR OF THE SOLAR PANEL

Fig. 2 and Fig. 3 illustrate the calculus diagram and the basic diagram of an equatorial solar tracker (where  $A_\phi$  and  $A_\omega$  are the linear actuators for the angular displacements  $\Phi$  and  $\omega$ , see Fig. 2). According to Fig. 2 and Fig. 3, in the  $X_0Y_0Z_0$  trihedron, result the following solar panel normal unit vector correlations: (7) for the equatorial dual-axis solar tracker unit vector (Fig.2), (8) for the azimuthal dual-axis solar tracker unit vector (Fig. 3), (9) for the horizontally fixed solar panel unit vector and (10) for solar panel sloped at  $\Phi = \phi - \delta$  (the angle between the solar panel normal unit vector and the zenital axis).

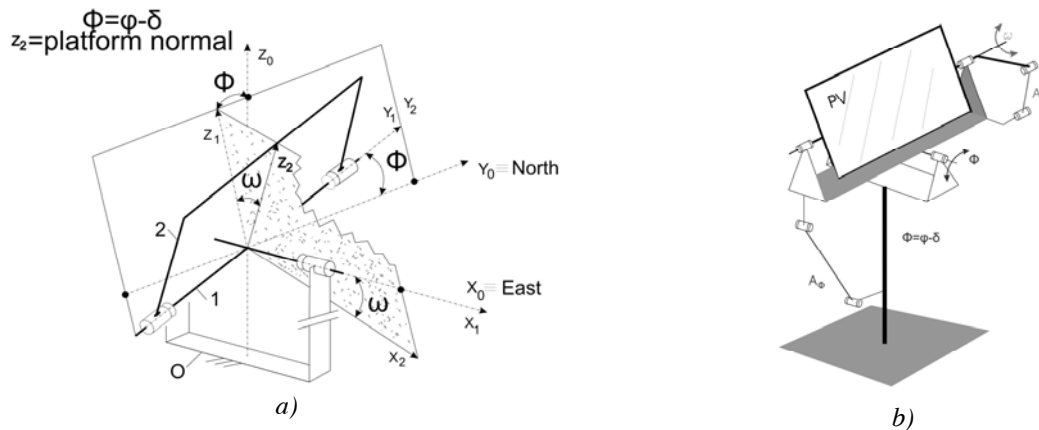


Figure 2. Equatorial Dual-Axis Tracker

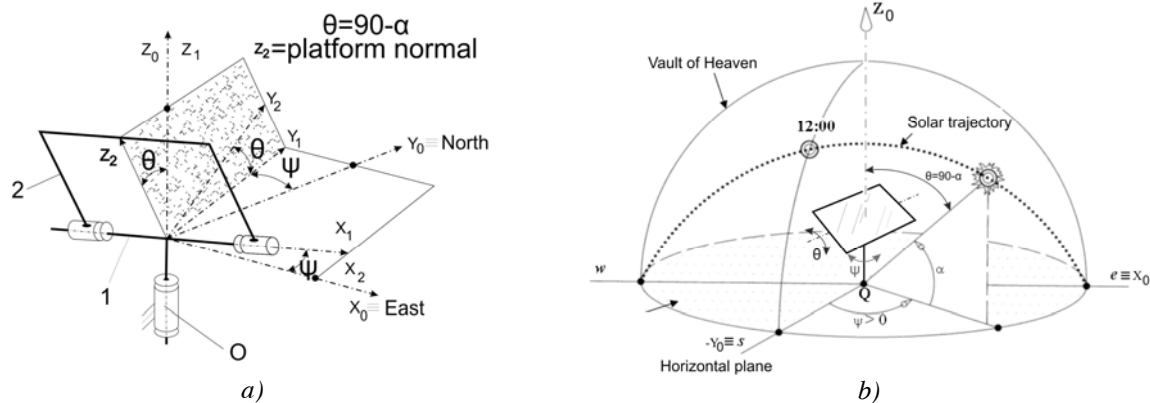


Figure 3. Azimuthal Dual-Axis Tracker

$$\bar{e}_{PV-eq} = [k_2]_{x_0, y_0, z_0} = \begin{bmatrix} \sin \omega \\ -\cos \omega \cdot \sin(\varphi - \delta) \\ \cos \omega \cdot \cos(\varphi - \delta) \end{bmatrix}; \bar{e}_{PV-az} = [k_2]_{x_0, y_0, z_0} = \begin{bmatrix} \cos \alpha \cdot \sin \psi \\ -\cos \alpha \cdot \cos \psi \\ \sin \alpha \end{bmatrix} \quad (7),(8)$$

$$\bar{e}_{PV-fix-horiz} = [k_2]_{x_0, y_0, z_0} = \begin{bmatrix} 0 \\ 0 \\ 1 \end{bmatrix}_{x_0, y_0, z_0}; \bar{e}_{PV-fix-\delta} = [k_2]_{x_0, y_0, z_0} = \begin{bmatrix} 0 \\ -\sin(\varphi - \delta) \\ \cos(\varphi - \delta) \end{bmatrix}_{x_0, y_0, z_0} \quad (9),(10)$$

#### 4. THE INCIDENCE ANGLE MODELLING AND ITS SIMULATIONS

The angle of incidence correlations result from the dot product of the sun-ray unit vector (6) and:

- a) the solar panel normal unit vector for the equatorial solar tracker (7), b) the solar panel normal unit vector for the azimuthal solar tracker (8), c) the horizontally fixed solar panel normal unit vector (9), d) the sloped solar panel normal unit vector (10):

$$\cos v = \bar{e}_{sun-ray} \cdot \bar{e}_{PV-eq} = \quad (11)$$

$$= \cos \alpha \cdot \sin \psi \cdot \sin \omega^* + \cos \alpha \cdot \cos \psi \cdot \cos \omega^* \cdot \sin(\varphi - \delta) + \sin \alpha \cdot \cos \omega^* \cdot \cos(\varphi - \delta)$$

$$\cos v = \bar{e}_{sun-ray} \cdot \bar{e}_{PV-az} = \quad (12)$$

$$= \cos \alpha \cdot \sin \psi \cdot \cos \alpha^* \cdot \sin \psi^* + \cos \alpha \cdot \cos \psi \cdot \cos \alpha^* \cdot \cos \psi^* + \sin \alpha \cdot \sin \alpha^*$$

$$\cos v = \bar{e}_{sun-ray} \cdot \bar{e}_{PV-fix-horiz} = \sin \alpha = \cos \theta \quad (13)$$

$$\cos v = \bar{e}_{sun-ray} \cdot \bar{e}_{PV-fix-\delta} = \cos \alpha \cdot \cos \psi \cdot \sin(\varphi - \delta) + \sin \alpha \cdot \cos(\varphi - \delta) \quad (14)$$

By economic reasons, the mobile panels displacement is made discontinuously (in steps); therefore, in the correlations (11) and (12) the solar panel variables have discrete variation and are marked with asterisk:  $\omega^*$ ,  $\psi^*$  and  $\alpha^*$  (in order to distinguish them from the sun-ray variables, which have continuous variation:  $\omega$ ,  $\psi$  and  $\alpha$ ).

Using the previous correlations, there were made numerical simulation, considering as input data:  $\varphi = 37^\circ$  N, day  $n=172$  Summer Solstice (June 21st)  $\Leftrightarrow \delta \approx +23,45^\circ$ , an orientation cycle of the solar panel consists in: aprox. 1 min. displacement + aprox. 59 min. standing. Some of the simulations' results, made with Excel Software, are illustrated in Fig. 4, 5 and 6.

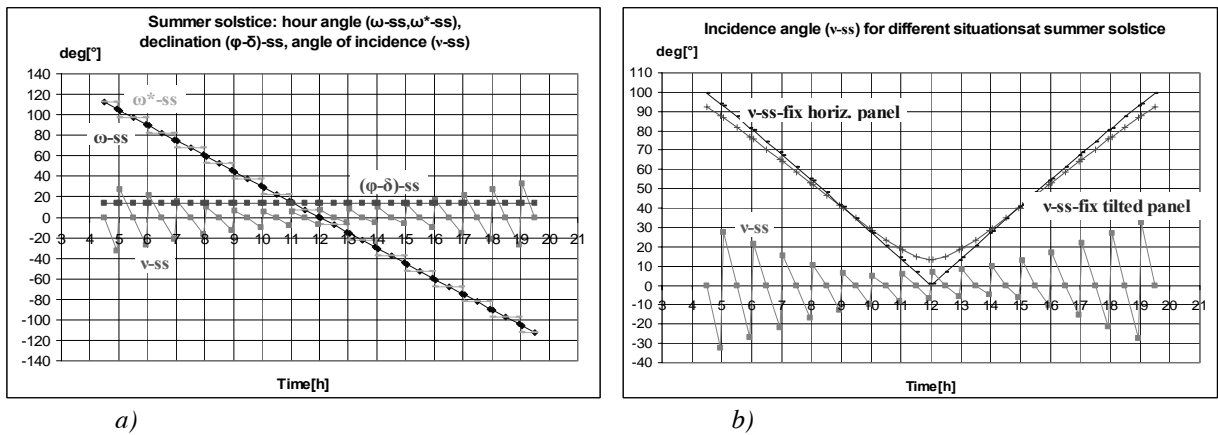
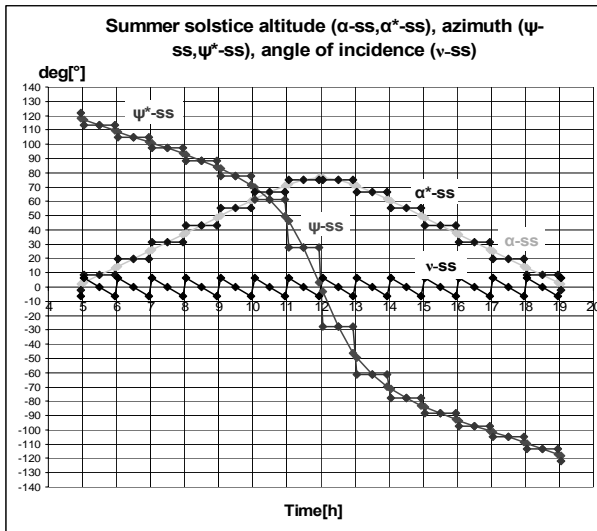
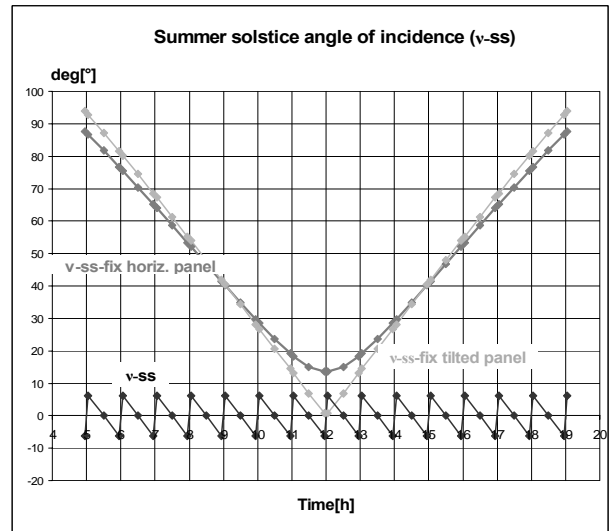


Figure 4. Summer solstice variations of  $\omega$ ,  $\omega^*$ ,  $\Phi = \Phi^*$  and  $v$  for an equatorial dual-axis tracker (a) and variation of the incidence angle  $v$  for an equatorial dual-axis tracker vs. a horizontally fixed solar panel and a sloped solar panel (b).

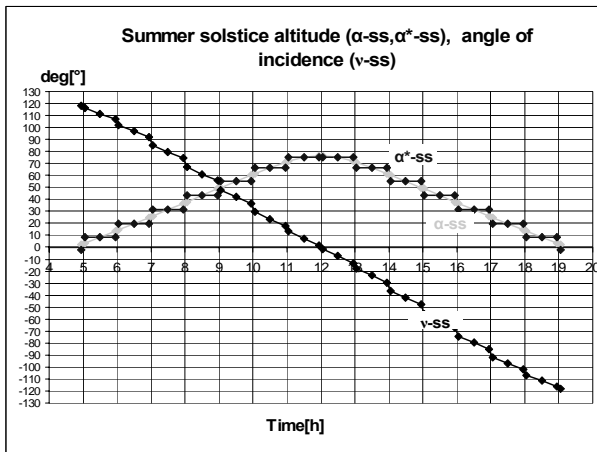


a)

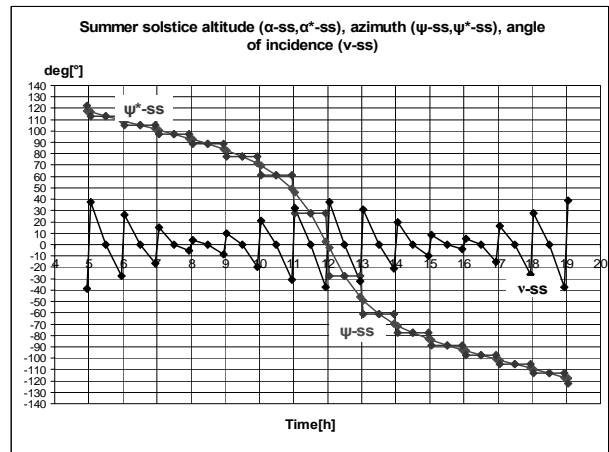


b)

Figure 5. Variations of  $\psi$ ,  $\psi^*$ ,  $\alpha$ ,  $\alpha^*$ ,  $v$  for an azimuthal dual-axis tracker (a) and  $v$  variation for an azimuthal dual-axis tracker vs. a horizontally fixed solar panel and a sloped solar panel (b).



a)



b)

Figure 6. Summer solstice for  $\alpha$ ,  $\alpha^*$  and  $v$  for an azimuthal single-axis tracker with  $\psi^*=0$  (a) and variation of  $\psi$ ,  $\psi^*$  and for an azimuthal single-axis solar tracker with  $\alpha^* = \text{constant} \approx 40^\circ$  (b)

## 5. CONCLUSIONS

- In the considered numerical situation, the fixed solar panels have incidence angles similar variations (see Fig.4,b and 5,b) and comparable with the single-axis azimuthal solar tracker variation with  $\psi^*=0$  (see Fig.6,a).
- The minimal incidence angles are achieved with the dual-axis azimuthal solar tracker (see Fig. 5); but this tracker type is less economic.
- During a day, the dual-axis equatorial tracker works practically in single-axis operation mode and achieves more reduced incidence angles around noon (see Fig.4); a significant improvement can be achieved if the time step is smaller in the morning and in the evening.
- Azimuthal solar tracker with  $\alpha^* \approx 40^\circ = \text{constant}$  (see Fig.6,b) works in single axis operation mode and achieves incidence angles similar to the equatorial tracker incidence angles ( except from noon); as a conclusion, the azimuthal displacement has a much higher influence compared to the altitudinal displacement.

## 6. REFERENCES

- Messenger, R., Ventre, J.: Photovoltaic System Engineering, London, CRC Press, 2000.
- Diaconescu, D. a.o.: Analysis of the Sun-Earth angles used in the design of the solar collectors' trackers, Bulletin of the Transilvania University of Brasov, Vol.13(47), 2006, pg. 99-105.